Higher Order Polarization Density in Gyrokinetics

Xishuo Wei,[1, 2] Yueyan Li,[3,2,4] and Yong Xiao[2, a)]

[1)] *Department of Physics and Astronomy, University of California, Irvine.*
[2)] *Institute for Fusion Theory and Simulation, Department of Physics, Zhejiang University*
[3)] *Center for Nonlinear Plasma Science and C.R. ENEA Frascati, Frascati, Italy*
[4)] *CREATE Consortium, Napoli, Italy*
a) Electronic email: yxiao@zju.edu.cn

Abstract

High confinement fusion plasmas feature strong gradient pedestal, where extra polarization density due to steep gradient needs to be considered in gyrokinetic simulation and a numerical scheme based on Padé approximation is invented to include this higher order polarization. The physics consequences of this polarization correction are investigated via gyrokinetic simulation on the ion temperature gradient mode instability and turbulence. It is discovered that this higher order polarization can affect the mode structure significantly and thus nonlinear turbulent transport.

I. INTRODUCTION

Gyrokinetic theory has been extensively used in the theoretical and computational studies of fusion plasmas [1-3]. The gyrokinetic Vlasov equation describes the single particle motion in gyrocenter phase space. The gyrokinetic field equations, on the other hand, need to be solved for the field quantities in original phase space. The polarization density and current account for the density and current change during the phase space transformation. In the electrostatic case, the polarization density in the Poisson equation comes from the averaged particle position shift in the direction of perturbed electric field. Dubin et al. have originally derived an analytic expression for the polarization density using modern gyrokinetic theory [4]. In this derivation, the conventional polarization density is kept to the order of $k_\perp^2\rho^2$ with a higher order correction in the order of $k_\perp\rho^2/L_n$, where L_n is the scale length of the equilibrium density with $L_n = \left(\frac{1}{n}\frac{dn}{dr}\right)^{-1}$. For low confinement plasmas, the density scale length L_n is much larger than perpendicular wavelength $1/k_\perp$. So the higher order correction is much smaller than the leading order term, and is often neglected in conventional gyrokinetic studies of core plasmas [5-7].

However, it is advantageous for fusion plasmas to be operated in high confinement mode (H-mode), which is designed to be the main operating scenario for ITER [8]. There have been keen interests in simulating turbulent transport for the H mode pedestal plasmas [9, 10], where the higher order polarization can be as important as the conventional leading order polarization while the gyrokinetic ordering still persists. Therefore, the gyrokinetic model needs to be carefully reviewed to include this higher order correction when simulating the pedestal plasmas. Important issues in this subject include adapting the Poisson equation to steep gradient plasmas, design and implement appropriate numerical scheme in the gyrokinetic simulation, as well as investigating associated prominent physics effects.

In this work, we investigate the effect of the higher order polarization term via gyrokinetic theory and simulation and use ion temperature gradient (ITG) mode [11] as an example to demonstrate the physics consequence of this higher order term. Two different approaches, namely the initial value method in ballooning space and global particle simulation in toroidal geometry, are utilized to study the ITG mode physics for strong density gradient and weak gradient case, respectively. For both cases, the linear growth rate of ITG instability is insensitive to

the higher order polarization, but the mode structures show visible change due to the polarization correction. In the ballooning space, an anti-symmetric high order correction is induced by the polarization correction. The kinetic electron response is found to magnify the high order polarization effect. In the GTC simulation, the change in the growth rate for different eigenmodes can make the most unstable mode jump from one eigenmode to another one, resulting in totally different mode structure. In the GTC nonlinear simulations, the high order polarization density is found to decrease the radial transport.

This paper is organized as follows: In Section II, we introduce the gyrokinetic model to explain the origin of high order polarization density. In Section III, the high order polarization effect in ballooning space is presented. The implementation of corrected Poisson equation in real space used in GTC is described in Section IV and the GTC simulation results are provided in Section V.

II. GYROKINETIC FOMULATIONS WITH HIGH ORDER POLARIZATION DENSITY

In collisionless limit, the evolution of distribution function $F_{GY}(\boldsymbol{R}, v_\parallel, \mu, t)$ in gyrocenter space $(\boldsymbol{R}, v_\parallel, \mu)$ is given by the Vlasov equation:

$$\frac{dF_{GY}}{dt} = \frac{\partial F_{GY}}{\partial t} + \dot{\mathbf{R}} \cdot \frac{\partial F_{GY}}{\partial \mathbf{R}} + \dot{v}_\parallel \frac{\partial F_{GY}}{\partial v_\parallel} = 0, \tag{1}$$

where $\boldsymbol{R}$ is the gyrocenter position, and μ is the magnetic moment. In the electrostatic limit, the time evolution of $(\boldsymbol{R}, v_\parallel)$ is given by the following equation of motion:

$$\dot{\mathbf{X}} = v_\parallel \hat{b} + \mathbf{v}_E + \mathbf{v}_d, \tag{2}$$

$$\dot{v}_\parallel = -\frac{1}{m}\frac{B^*}{B_\parallel^*}(q\nabla\langle\phi\rangle + \mu\nabla B), \tag{3}$$

where q and m are the charge and mass of the particle respectively, $\hat{b} = \boldsymbol{B}/B$ is the unit vector along the magnetic field, $\boldsymbol{B}^* = \boldsymbol{B} + Bv_\parallel \nabla \times \hat{b}/\Omega_c$, $B_\parallel^* = \boldsymbol{B}^* \cdot \hat{b}$. $\boldsymbol{v}_E$ is the $\boldsymbol{E} \times \boldsymbol{B}$ drift, $\boldsymbol{v}_d$ is the magnetic drift. These drift velocities take the following form:

$$\boldsymbol{v}_E = \frac{\hat{b} \times \nabla\langle\phi\rangle}{B_\parallel^*}, \tag{4}$$

$$\boldsymbol{v}_d = \frac{1}{ZeB_\parallel^*}\left[mv_\parallel^2 \hat{b} \times \left(\hat{b} \cdot \nabla\hat{b}\right) + \mu\hat{b} \times \nabla B\right], \tag{5}$$

where and the gyro-averaged electric potential $\langle\phi\rangle$ can be evaluated by,

$$\langle\phi\rangle = \int_0^{2\pi} \frac{d\alpha}{2\pi} \int \phi(\mathbf{x})\delta(\mathbf{x} - \mathbf{R} - \boldsymbol{\rho})d\mathbf{R}, \tag{6}$$

where α is the gyro-phase, $\boldsymbol{\rho} = \boldsymbol{v} \times \hat{b}/\Omega_c$ is the gyro-radius, and $\Omega_c = ZeB/m$ is the particle's gyro-frequency.

For wave lengths larger than the Debye length, the gyrokinetic Poisson's equation based on quasi-neutrality is used to close the gyrokinetic system, $\mathrm{n_i}(\boldsymbol{x}) = n_e(\boldsymbol{x})$. Note that the particle density is expressed in particle position space. However, it is not convenient to calculate the particle density in gyrokinetic simulations. Instead, the "gyrocenter density" is convenient to calculate,

$$\bar{n}(x) = \int d^3v \int F_{GY}(\mathbf{R})\delta(\mathbf{R} - \mathbf{x} + \boldsymbol{\rho})d\mathbf{R}. \tag{7}$$

In the presence of electromagnetic fluctuations, the distance between particle position and gyrocenter is no longer a constant value ρ, which makes $\bar{n}$ different from the particle density $n(\boldsymbol{x})$. The difference between $n(\boldsymbol{x})$ and $\bar{n}(\boldsymbol{x})$ comes from the averaged particle position shift due to the electromagnetic fluctuations, which is termed polarization density,

$$n_{pol} = n(\mathbf{x}) - \bar{n}(\mathbf{x}). \tag{8}$$

Following the derivation in Refs. [12, 13], and assuming the gyrokinetic ordering $e\phi/T_e \ll 1$, $k_\parallel \ll k_\perp$, $\rho\ /L_B \ll 1$, we can obtain the relationship between particle distribution and gyrocenter distribution in the electrostatic limit:

$$f(x,v) = \int \left(1 + \frac{q_s}{B}\frac{\partial\widetilde{\Phi}}{\partial\theta}\frac{\partial}{\partial\mu}\right) F_{GY}(\mathbf{R}, v_\parallel, \mu)\delta(\mathbf{R} - \mathbf{x} + \boldsymbol{\rho})d\mathbf{R}, \tag{9}$$

where $\widetilde{\Phi}$ is the mean deviation of gyro-averaged potential from the potential felt by the particle,

$$\widetilde{\Phi} = \int_\alpha d\alpha\ [\phi(\mathbf{R} + \rho) - \langle\phi\rangle(\mathbf{R})]\ \ d\mathbf{R}. \tag{10}$$

By Taylor expanding the gyrocenter distribution function and assuming the lowest order distribution to be Maxwellian, we obtain the leading order and the next order polarization density, i.e., $n_{pol} = n_{pol,1} + n_{pol,2}$ with

$$\begin{aligned} n_{pol,1} &= -\frac{Ze}{T} n_0 \phi_k [1 - \Gamma_0(b)], \\ n_{pol,2} &= -i\frac{Zen_0}{T}\rho_{th}^2 \mathbf{k}\cdot\nabla \ln n_0\ [-\Gamma_0(b) + (1 - \eta_i)\Gamma_1(b)]. \end{aligned} \tag{11}$$

which corresponds to the first two terms in the expansion of distribution function.

When deriving Eq. (11), we have transformed the physical quantities to Fourier space. Here, $\eta_i = dlnT_i/dlnn_0$, $\Gamma_n(b) = I_n(b)e^{-b}$, and I_n is the n-th order modified Bessel function, $b = k_\perp^2\rho_i^2$, $\rho_i = \sqrt{m_i T_i}/(q_i B)$. If we neglect the effect of non-uniform temperature, the second order polarization density $n_{pol,2}$ would be identical to the results in Ref.[4]. In this work, we also focus on the effect of non-uniform density by temporarily assuming a weak temperature gradient.

The first order polarization term is widely used in gyrokinetic simulation [14]. However, the second order polarization term only becomes important in the presence of steep density gradient. The quasi-neutrality condition with these two polarization terms is then given by

$$\frac{Z_i e n_0}{T_i}[1 - \Gamma_0(b)]\phi_k + i\frac{Z_i e n_{0i}}{T_i}\rho_i^2 \mathbf{k}\cdot\nabla \ln n_0\ [-\Gamma_0(b) + (1 - \eta_i)\Gamma_1(b)]\phi_k = Z_i e\bar{n}_{ik} - en_{ek}, \tag{12}$$

where the electron polarization density is neglected because the electron gyro-radius is much smaller than the ion gyro-radius. Note that in the long wave length limit, the second order polarization density reduces to $-i\boldsymbol{k}\cdot\frac{\nabla n_0\phi_k Z_i^2 e^2}{T_i} \sim -\nabla n_0\cdot\nabla\phi Z_i^2 e^2/T_i$, which is also used in some gyrokinetic models and simulations [15, 16] as the correction to Poisson's equation with density non-uniformity.

In the small gyro-radius limit, $k_\perp\rho_{th} \ll 1$, the ratio between the two polarization densities $n_{pol,2}/n_{pol,1} \sim 1/$

$(\boldsymbol{k}\cdot\boldsymbol{L}_n)$. For most studies in the tokamak's core region, where the ratio between the background density scale length and the wavelength of the perturbed fields is small, the second or higher order polarization term can be ignored. However, in the region where the background particle density changes drastically, like the tokamak pedestal in the H-mode regime, $n_{pol,2}$ can be comparable to $n_{pol,1}$, as is shown in Fig. 1. The second order polarization must be considered seriously in both theory and simulation, especially for those modes with $\mathrm{k}_\perp\rho_i < 1$ and $k_r L_n \sim 1$.

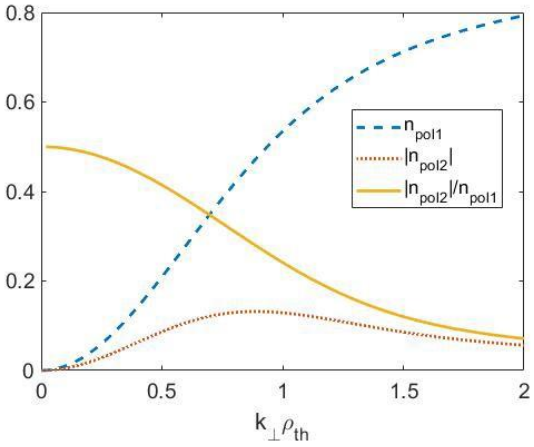

Fig. 1 Comparison of two polarization densities: $n_{pol,1}$ and $n_{pol,2}$ in Eq. (11) with $k_r L_n = 1$, which are normalized by $Z_i e\phi n_{\mathrm{n}}/T_i$

III. LOCAL SIMULATION WITH WEAK DENSITY GRADIENT

Although the higher order polarization density $n_{pol,2}$ is only important in the presence of steep density gradient, we can still start from the weak gradient to get an intuitive or qualitative picture about the tendency for its physics consequence. For the weak gradient case, since the polarization correction can only cause slight change in the mode structure and it is difficult to distinguish this effect in the GTC simulation due to the Monte Carlo particle noise, here we use a gyrokinetic simulation in the 1D ballooning space, to capture the subtle variation in the mode structure. When the density gradient in a tokamak is relatively small, $k_r L_n \ll 1$, the ballooning representation is valid in the local limit for high n modes. From the 1D simulation in ballooning space, we illustrate the consequence of the new polarization $n_{pol,2}$ for the weak density gradient case, which implies a more significant role for $n_{pol,2}$ when the density gradient becomes steep. The governing equation for the ion guiding center distribution function is given by

$$\frac{\partial \mathrm{g}}{\partial t} = -\frac{v_\parallel}{q}[\partial_\theta g + J_0 F_0 \partial_\theta \phi + (\partial_\theta J_0) F_0 \phi] - i\omega_D \mathrm{g} + (i\omega_{*T} - \omega_D) J_0 F_0 \phi, \tag{13}$$

where $J_0 = J_0(b)$ with $b = k_\perp^2 \rho_i^2$, $g \equiv h - J_0 F_0 \phi$, and h is the non-adiabatic part of the perturbed ion distribution function, and the first order distribution function $\delta f_i = h - n_0 q_i \phi / T_i$, θ is the ballooning angle, F_0 is the equilibrium distribution function or simply Maxwellian. In addition, ω_D is the drift frequency,

$$\omega_D = 2\frac{L_n}{R_0}\omega_{*i}[\cos\theta + \hat{s}\theta\sin\theta]\left(v_\perp^2/2 + v_\parallel^2\right)/\left(2v_{th,i}^2\right), \tag{14}$$

where $\hat{s}$ is the magnetic shear, $\omega_{*T} = \omega_{*i}[1 + \eta_i(E/T_i - 3/2)]$ with $\omega_{*i} = -k_\theta T_i/(Z_i e B L_n)$. The quasi-neutrality condition yields

$$\int g d^3v = \frac{en_0}{T_e}\phi + \frac{Z_i en_0}{T_i}\big(1-\Gamma_0(b)\big)\phi + i\frac{Z_i en_0}{T_i}\frac{k_r\rho_i^2}{L_n}\big(\Gamma_1(b)-\Gamma_0(b)\big)\phi, \tag{15}$$

where the second order polarization has been included in this equation.

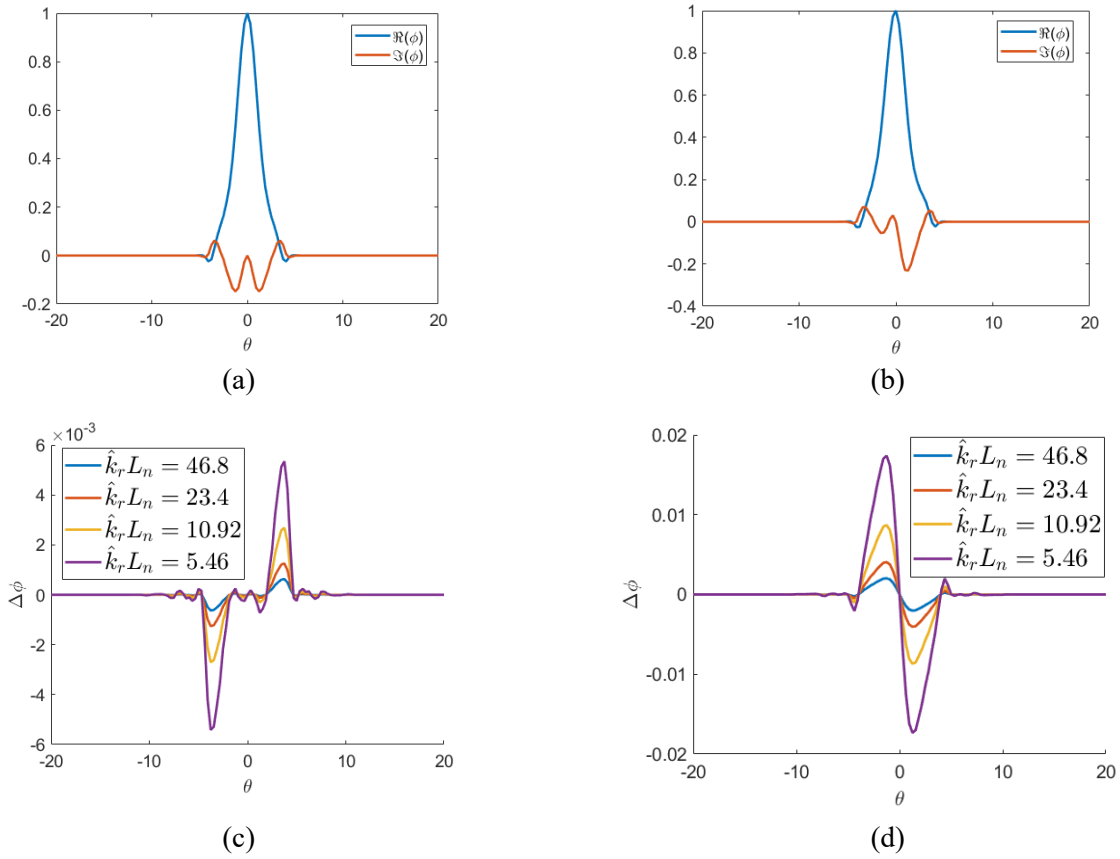

Fig. 2 The effect of second order polarization on ITG eigenmode structure. (a) the mode structure excluding $n_{pol,2}$. (b) the mode structure including $n_{pol,2}$. (c) real part of the mode structure change for different values of $k_r L_n$. (d) imaginary part of mode structure change for different values of $k_r L_n$. It is noted that $k_r L_n = \hat{k}_r L_n \theta$.

The gyrokinetic simulations of this model system are carried out for typical ion temperature gradient (ITG) instability, with simulation parameters set as $\varepsilon \equiv r/R_0 = 0.2$, $T_i = T_e$, $L_n = 0.2R_0$, $\eta_i = 3.114$, $q = 1.4$, $\hat{s} = 0.78$, and if not specifically mentioned, $k_\theta L_n = 14$. As one would expect from the ordering estimate, the simulation shows that the weak density gradient has very little effect on the mode frequency and growth rate. But the change of eigenmode structure in the ballooning space can be explicitly observed even with this weak density gradient, as is shown in Fig. 2. The normalized eigenmodes structure is plotted in Figure 2(a) & (b), from which we can see that the original even symmetric mode structure is tilted around the ballooning angle $\theta \sim 0$, where the unstable mode has the largest magnitude. From Figure 2(c) and (d), we can see that both real part and imaginary part of the mode structure could be affected, but the effect on imaginary part is more significant with these parameters and the effect on the real part is minimal. Not surprisingly, the effect of the second order polarization density is stronger for smaller $k_r L_n$ or larger density gradient, as we vary the value of $k_r L_n$ in Fig. 2(c)&(d). However, the overall effect is subdominant, since $k_r L_n = \hat{k}_r L_n \theta \propto k_\theta L_n \hat{s}\theta$, and thus the correction itself is small near $\theta \sim 0$.

IV. NUMERICAL IMPLEMENTATIONS OF GLOBAL GYROKINETIC SIMULATION

As we have discussed in Sec. II, the higher order polarization may become prominent for the pedestal plasma that possesses steep gradient. For the steep gradient case, the ballooning representation is no longer valid and we ought to use the global 3D gyrokinetic simulation code GTC [14, 17, 18] to investigate the higher order polarization effect on the ITG turbulence. In the GTC code, the gyrokinetic model is used for ions to treat ion scale turbulence. The drift kinetic model is used for electrons, and we can switch freely between adiabatic electron model and fluid-kinetic hybrid electron model [17]. The gyrokinetic Poisson's equation can be solved in real space by four-point averaging method [6] or Padé approximation [6, 19]. In this paper, we choose the Padé approximation for its convenience to implement the steep gradient effect caused by the higher order polarization. As for the Padé approximation, the bracket in the first term in Eq.(12), $1-\Gamma_0(b)$, is approximated by $k_\perp^2\rho_i^2/\left(1+k_\perp^2\rho_i^2\right)$. And similarly, the bracket in second term, $\Gamma_1(b)-\Gamma_0(b)$, can be approximated by $-1/\left(1+k_\perp^2\rho_i^2\right)^2$, as is shown in Fig. 3. Then we can rewrite Eq.(12) in the real space,

$$-\frac{Z_i^2e^2n_0}{T_i}\frac{\rho_i^2\nabla_\perp^2}{1-\rho_i^2\nabla_\perp^2}\phi-\frac{Z_i^2e^2n_0}{T_i}\frac{\rho_i^2\nabla\ln n_0}{1-\rho_i^2\nabla_\perp^2}\cdot\nabla_\perp\phi=Z_ie\delta\bar{n}_i-e\delta n_e. \tag{16}$$

A more compact but approximate form is given by

$$-\frac{Z_i^2e^2n_0}{T_i}\frac{\rho_i^2\frac{1}{n_0}\nabla\cdot(n_0\nabla_\perp)}{1-\rho_i^2\frac{1}{n_0}\nabla\cdot(n_0\nabla_\perp)}\phi=Z_ie\delta\bar{n}_i-e\delta n_e. \tag{17}$$

The left hand side of Eq.(17) has a form similar to the first term in the left hand side of Eq.(16). When the density gradient is weak, $|\nabla n_0|/n_0\ll|\nabla\phi|/\phi$, we can recover the classical Poisson's equation. From the perspective of numerical simulation, we can simply replace the original Laplacian operator $\nabla_\perp^2$ in the classical Poisson solver with the new operator $\widetilde{\Delta}\equiv 1/n_0\nabla\cdot(n_0\nabla_\perp)=\nabla_\perp^2+(\nabla\,ln\,n_0)\cdot\nabla_\perp$. The simulation is carried out in the magnetic flux coordinate system [19]. Since the equilibrium density depends solely on poloidal magnetic flux ψ, the operator correction is further expressed as $\left(\partial_\psi\,ln\,n_0\right)\left(g^{\psi\psi}\partial_\psi+g^{\psi\theta}\partial_\theta+g^{\psi\zeta}\partial_\zeta\right)$, where the geometric coefficients $g^{\psi\psi}$, $g^{\psi\theta}$ and $g^{\psi\xi}$, corresponds to the different components of the geometric tensor with $g^{XY}=\nabla X\cdot\nabla Y$. The detailed derivation and implementation are given in Appendix B.

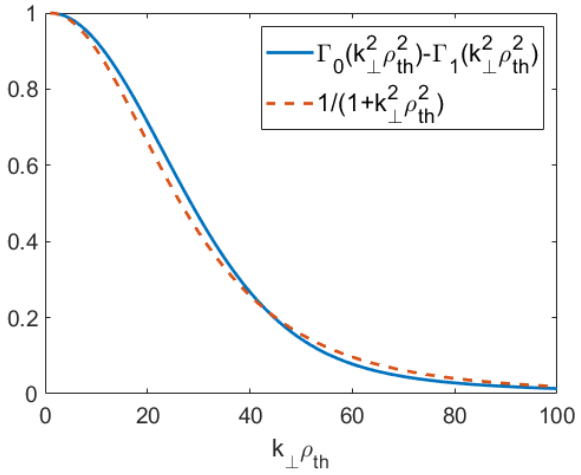

Fig. 3. Padé approximation of $\Gamma_0-\Gamma_1$.

v. RESULTS FROM GTC SIMULATION

Next we carry out gyrokinetic simulations with steep gradients using the GTC code for the ITG instability to observe the effects of higher order polarization correction. The following parameters are used for the simulation: $T_i = T_e = 2.2$ keV, $n_e = 8.93 \times 10^{18}$ m^{-3}, $L_{Ti}/R_0 = 0.040, L_{Te}/R_0 = 0.040, L_n/R_0 = 0.027$, $k_r L_n \sim 2$, $q = 1.4$, $\hat{s} = 0.78$. The adiabatic electrons are assumed in the simulation to exclude kinetic electron effects for simplicity in the beginning. We use a concentric circular cross section tokamak for the simulation. The equilibrium profiles are given in the analytical formulations [20], in which a number of control coefficients can be adjusted to change the plasma profile and the associated gradients and thus the nature of the instability can be adjusted as well.

It turns out that the simulation shows negligible change in the linear frequency and growth rate change from the high order polarization density. The poloidal mode structures are shown in Fig. 4(a) & (b) for cases with and without the second order polarization density. We can see only a slight change in linear mode structure for the ITG instability. The nonlinear heat conductivity is found decreased after the correction of the second order polarization, as is shown in Fig. 4(c). When the kinetic electron response is included, the effect of the higher order polarization effect is amplified, as can be seen in Fig. 5. Although the linear growth rate is only slightly changed, the poloidal mode structure shows significant rotation in Figs. 5(a) & (b). That means the higher order polarization correction provides visible modulation on the fast growing eigenmodes, and some different eigenmode becomes the most unstable one with the correction. Note that in the ITG simulation with adiabatic electrons, the electron response is much larger than the ion polarization, meaning that the potential change can be shielded by the adiabatic electron response in a large degree. While in the simulation with kinetic electron response, the shielding from the electrons is weaker, which makes important the total ion polarization and then the higher order ion polarization as well.

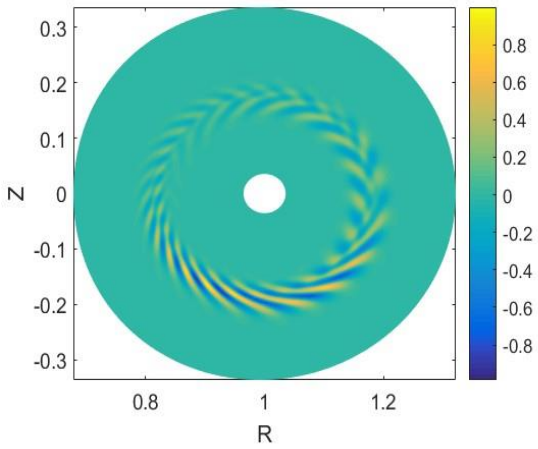

(a)

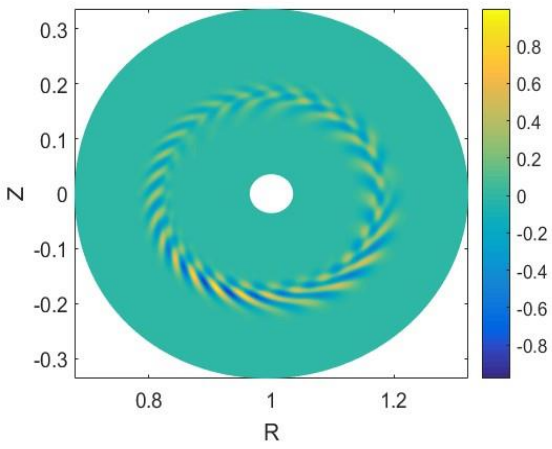

(b)

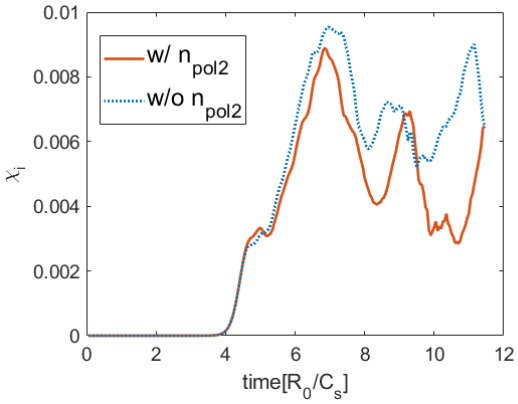

(c)

Fig. 4. ITG simulation with adiabatic electrons for high order polarization correction: (a) 2D mode structure on poloidal plane using traditional Poisson's equation; (b) 2D mode structure on poloidal plane using modified Poisson's equation with higher order polarization correction; (c) time evolution of heat conductivity with and without the higher order polarization correction.

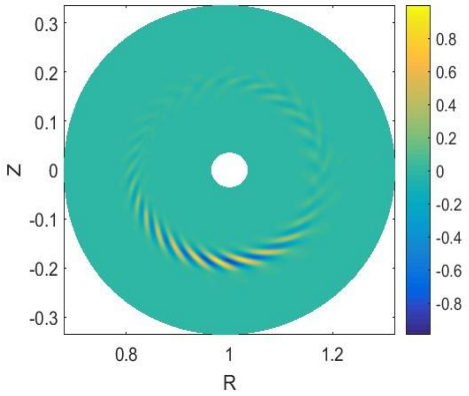

(a)

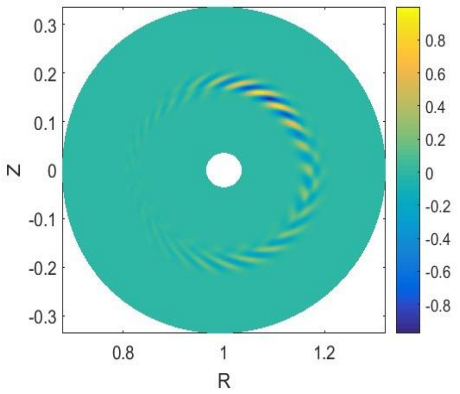

(b)

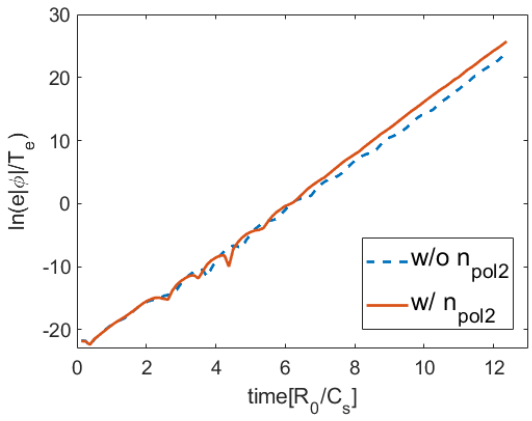

(c)

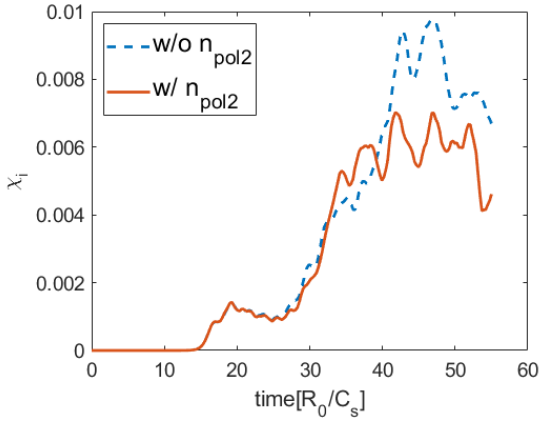

(d)

Fig. 5. 2D structure of ITG mode with kinetic electron response on the poloidal plane calculated by GTC: (a) traditional Poisson's equation; (b) modified Poisson's equation. (c) Comparison of the linear growth of the ITG mode for cases

with and without higher order polarization. (d) Comparison of nonlinear ITG heat transport for cases with and without higher order polarization.

VI. Conclusion

In this work, we have demonstrated the effect of high order ion polarization density effect in the gyrokinetic simulation. The theoretical analysis shows the ratio between high order polarization density and conventional polarization density is in the order of $1/k_r L_n$, which means both terms are equally important and thus need to be considered on an equal footing in steep density gradient regime. We compared the ITG mode in the ballooning space simulations and global gyrokinetic simulation using GTC to illustrate the effect of the higher order polarization correction. In the global GTC simulations, the ITG frequency and growth rate is found insensitive to the higher order polarization correction and the mode structure change due to this correction is more visible. We find that in the local 1D ballooning space simulation, the high order correction induces an anti-symmetric structure for the linear ITG mode. The nonlinear GTC simulation shows the radial heat transport is suppressed when the high order polarization is considered. The simulation with kinetic electron response is affected more significantly by the high order correction, because the weaker shielding effect from adiabatic response. In certain parameter regime, the higher order correction can lead to a rotation for the poloidal mode structure, as demonstrated by the global ITG simulation with kinetic electrons. The nonlinear simulation further shows that the rotation of the linear mode structure can suppress the turbulent transport.

Appendix A: Derivation of polarization density in electrostatic limit

Here we basically follow the derivation in the modern gyrokinetic theory [12, 21-23] to derive the polarization density under steep gradient. The preliminary transformation is from the normal $(\mathbf{x}, \mathbf{v})$ Cartesian coordinates to $(\boldsymbol{x}, \mu, v_\parallel, \alpha)$, where we can write the Lagrangian 1-form in the new phase space as

$$\Gamma = \left(e\mathbf{A} + mv_\parallel \hat{b} + mv_\perp \hat{n}_\perp\right) \cdot d\mathbf{x} - \left(\frac{1}{2}mv_\parallel^2 + \mu B\right) dt. \tag{18}$$

Note that both the symplectic part of the Lagrangian involves fast gyromotion oscillations. Given the normal gyrokinetic ordering, $\epsilon_B = \rho/L_B \ll 1$, we can use the Lie-transformation in the phase space to eliminate the fast gyromotion oscillation in the Lagrangian, and to the leading order, the new guiding center Lagrangian is given by

$$\Gamma_{GC} = \left(e\mathbf{A}(\mathbf{X}_{GC}) + m\mathbf{v}_{\parallel,GC}\right) \cdot d\mathbf{X}_{GC} - \mu_{GC}\frac{m}{e}d\theta_{GC} - \left(\frac{1}{2}mv_{\parallel,GC} + \mu_{GC}B\right) dt, \tag{19}$$

where the subscription GC stands for 'guiding center space'. The transformation is simply $\boldsymbol{X}_{GC} = \boldsymbol{x} + \boldsymbol{\rho}$, and any functions of $\mathbf{x}$ should also be transformed $f(\boldsymbol{x}) \rightarrow F_{GC}(\boldsymbol{X}_{GC}) = exp[-\boldsymbol{\rho} \cdot \nabla] f(\boldsymbol{X}_{GC})$.
When the electrostatic perturbation enters the system, an additional term is added to the Hamiltonian part

$$\Gamma_{GC} = \left(e\mathbf{A}(\mathbf{X}_{GC}) + m\mathbf{v}_{\parallel,GC}\right) \cdot d\mathbf{X}_{GC} - \mu_{GC}\frac{m}{e}d\theta_{GC} - \left(\frac{1}{2}mv_{\parallel,GC} + \mu_{GC}B + e\phi_{GC}\right) dt. \tag{20}$$

Note that the $\phi_{GC} = \phi(\boldsymbol{X}_{GC} - \boldsymbol{\rho})$ induces another fast oscillation as well, despite that $\phi(\boldsymbol{x})$ is a slowly varying quantity. Another transformation from guiding center space to gyrocenter space can be performed to eliminate the fast gyromotion oscillations. Here because the perturbation only appears in the Hamiltonian part, we can write the new Lagrangian in which the symplectic part functional form remains unchanged,(i.e. The Hamiltonian representation in [13], and the new Lagrangian in the extended gyrocenter phase space is given by

$$\Gamma_{GY} = \left(e\mathbf{A_0}(\mathbf{X}_{GY}) + m\mathbf{v}_{\parallel,GY}\right)\cdot d\mathbf{X}_{GY} - \mu_{GY}\frac{m}{e}d\theta_{GY} - w_{GY}dt \\ -\left(\frac{1}{2}mv_{\parallel,GY} + \mu_{GY}B + e\langle\phi_{GC}(\mathbf{X}_{GY},t)\rangle - w_{GY}\right)d\tau, \tag{21}$$

where w_{GY} is the energy coordinate, and τ is the time-like Hamiltonian orbit variable, $\langle\phi_{GC}\rangle$ is the gyrophase averaging of the perturbed potential in "guiding center space", $\langle\phi_{GC}\rangle = 1/2\pi \times \int d\theta_{GC}\phi(\mathbf{x}+\boldsymbol{\rho})$. Since we carry out the transformation from particle space to guiding center space, and then the transformation from guiding center space to gyrocenter space, we can write out the relation between the distribution function in particle space and that in the gyrocenter space. Considering the orderings $k_\parallel \ll k_\perp, \rho \ /L_n \ll 1$, we have the following relation to the first order

$$f = e^{\boldsymbol{\rho}\cdot\nabla}F_{GY} + e^{\boldsymbol{\rho}\cdot\nabla}\left(\frac{e}{T}\left(\phi(\boldsymbol{x}-\boldsymbol{\rho}) - \bar{\phi}(\boldsymbol{x})\right)F_{GY}\right). \tag{22}$$

Note the operator $e^{\boldsymbol{\rho}\cdot\nabla}$acts on both perturbed and equilibrium quantities in the bracket. In the Fourier space, we assume the angle between $\mathbf{k}$ and $\boldsymbol{\rho}$ is α without losing generality. The perturbed quantities in the second term of Eq.(22) related to the potential is

$$e^{\rho\cdot\nabla}\left(\phi(\boldsymbol{x}-\boldsymbol{\rho}) - \bar{\phi}(\boldsymbol{x})\right) \to \exp(ik_\perp\rho\sin\alpha)\,[\phi_k\exp(-ik_\perp\rho\sin\alpha)] \\ = \phi_k - J_0(k_\perp\rho)\phi_k\exp(ik_\perp\rho\sin\alpha). \tag{23}$$

Assume that the angle between $\mathbf{k}$ and ∇F_{GY} is φ and the angle between $\boldsymbol{\rho}$ and ∇F_{GY} is $\alpha+\varphi$. The equilibrium part to the first order of ρ/L_n in the second term of Eq.(22) is

$$exp(\boldsymbol{\rho}\cdot\nabla)\left(\frac{e}{T}F_{GY}\right) = F_{GY} + F_{GY}\rho\left|\nabla\left(\frac{e}{T}ln\,F_{GY}\right)\right| sin(\alpha+\varphi). \tag{24}$$

Neglecting the nonlinear effect in the transformation by only keeping equilibrium part of F_{GY} in Eq.(22) and further assuming the zeroth order of F_{GY} is Maxwellian distribution, we can obtain the expression for f

$$f_k = e^{ik_\perp\rho\,sin\,\alpha}F_{GY,k} + \left(\phi_k - J_0(k_\perp\rho)\phi_k e^{ik_\perp\rho\,sin\,\alpha}\right)\times \\ \left(F_m + F_m\rho|\nabla\,ln\,n|\left[1+\eta\left(\frac{mv^2}{2T}-\frac{5}{2}\right)\right]sin(\alpha+\varphi)\right). \tag{25}$$

The polarization density is obtained by integrating the second part of Eq.(24), and it can be separated to two terms corresponding to the two terms in Eq.(23) .

$$n_{pol,1} = \int d^3v\left(\phi_k - J_0(k_\perp\rho)\phi_k e^{ik_\perp\rho\,sin\,\alpha}\right)F_M = -\frac{e}{T}n_0\phi_k[1-\Gamma_0(b)], \tag{26}$$

$$n_{pol,2} = \int d^3v\left(\phi_k - J_0(k_\perp\rho)\phi_k e_\perp^{ik\rho\sin\alpha}\right)F_M\rho|\nabla\ln n|\left[1+\eta\left(\frac{mv^2}{2T}-\frac{5}{2}\right)\right]\sin(\alpha+\varphi) \\ = -i\frac{e}{T}n_0\phi_k\rho_{th}^2k_\perp|\nabla\ln n_0|\cos\varphi\ \ [\Gamma_1(b)(1-\eta)-\Gamma_0(b)]. \tag{27}$$

When calculating $n_{pol,2}$, we have neglected $O\left(k_\perp^4\rho_{th}^4\right)$ terms, which is consistent with the edge plasma ordering. This new term of $n_{pol,2}$ is a correction to the polarization density associated with steep gradient.

Appendix B: Implementation of gyrokinetic Poisson equation with steep gradient

The steep gradient correction discovered in the Appendix A needs to be included in the gyrokinetic Poisson equation to simulate edge plasma physics accurately. For this purpose, we ought to implement numerically the operator $\widetilde{\Delta} \equiv 1/n_0 \nabla \cdot (n_0 \nabla_\perp) = \nabla_\perp^2 + (\nabla \ln n_0) \cdot \nabla_\perp$. In magnetic flux coordinates system (ψ, θ, ζ), and normally in equilibrium plasmas $\nabla \ln n_0 = \nabla\psi \partial_\psi n_0/n_0$ and correction is $(\nabla \ln n_0) \cdot \nabla_\perp = \kappa_n \left(g^{\psi\psi}\partial_\psi + g^{\psi\theta}\partial_\theta + g^{\psi\zeta}\partial_\zeta\right)$ and in 2D toroidal system, $g^{\psi\zeta} \approx 0$. In GTC code, we have developed a 11-point interpolation scheme to implement the perpendicular Laplacian operator $\nabla_\perp^2$ [19]. Fortunately, we already have the discrete forms for the differential operators such as ∂_ψ and ∂_θ. Therefore, we simply add the two additional terms at the relevant 11 points to implement the new $\widetilde{\Delta}$ operator with minimal modification to the original code. Because we explicitly consider the limit $k_\perp L_n \sim 1$, so the $\nabla_\perp$ operator and equilibrium quantities are no longer commutative. If we separate the electron density perturbation to the adiabatic response and non-adiabatic response. The gyrokinetic Poisson equation Eq. (16) becomes

$$-\frac{Z_i^2 n_i}{T_i}\frac{\rho_i^2\widetilde{\Delta}}{1-\rho_i^2\widetilde{\Delta}}\delta\phi + \frac{e^2 n_e}{T_e}\delta\phi = Z_i \delta\bar{n}_i - e\delta n_{e,k} \tag{28}$$

After some algebra, we obtain

$$-\rho_i^2\widetilde{\Delta}\delta\phi + \left(1-\rho_i^2\widetilde{\Delta}\right)\left(\frac{T_i}{Z_i^2 n_i}\frac{e^2 n_e}{T_e}\delta\phi\right) = \left(1-\rho_i^2\widetilde{\Delta}\right)\frac{T_i}{Z_i^2 n_i}\left(Z_i\delta\bar{n}_i - e\delta n_{e,k}\right) \tag{29}$$

Therefore, we can solve the electric potential by inverting the operator acting on $\delta\phi$ in the left hand side of the preceding equation.

Reference:

[1] P.J. Catto, W.M. Tang, D.E. Baldwin, GENERALIZED GYROKINETICS, Plasma Physics, 23 (1981) 639-650.

[2] E.A. Frieman, L. Chen, NON-LINEAR GYROKINETIC EQUATIONS FOR LOW-FREQUENCY ELECTROMAGNETIC-WAVES IN GENERAL PLASMA EQUILIBRIA, Physics of Fluids, 25 (1982) 502-508.

[3] W.W. Lee, GYROKINETIC APPROACH IN PARTICLE SIMULATION, Physics of Fluids, 26 (1983) 556-562.

[4] D.H.E. Dubin, J.A. Krommes, C. Oberman, W.W. Lee, NON-LINEAR GYROKINETIC EQUATIONS, Physics of Fluids, 26 (1983) 3524-3535.

[5] W.W. Lee, GYROKINETIC PARTICLE SIMULATION-MODEL, Journal of Computational Physics, 72 (1987) 243-269.

[6] Z. Lin, W.W. Lee, METHOD FOR SOLVING THE GYROKINETIC POISSON EQUATION IN GENERAL GEOMETRY, Physical Review E, 52 (1995) 5646-5652.

[7] S.E. Parker, W.W. Lee, A FULLY NONLINEAR CHARACTERISTIC METHOD FOR GYROKINETIC SIMULATION, Physics of Fluids B-Plasma Physics, 5 (1993) 77-86.

[8] ITER, https://www.iter.org/.

[9] P.B. Snyder, N. Aiba, M. Beurskens, R.J. Groebner, L.D. Horton, A.E. Hubbard, J.W. Hughes, G.T.A. Huysmans, Y. Kamada, A. Kirk, C. Konz, A.W. Leonard, J. Lonnroth, C.F. Maggi, R. Maingi, T.H. Osborne, N. Oyama, A. Pankin, S. Saarelma, G. Saibene, J.L. Terry, H. Urano, H.R. Wilson, Pedestal stability comparison and ITER pedestal prediction, Nuclear Fusion, 49 (2009).

[10] X.Q. Xu, M.V. Umansky, B. Dudson, R.B. Snyder, Boundary Plasma Turbulence Simulations for Tokamaks, Communications in Computational Physics, 4 (2008) 949-979.

[11] W. Horton, Drift waves and transport, Reviews of Modern Physics, 71 (1999) 735-778.

[12] T.S. Hahm, W.W. Lee, A. Brizard, NONLINEAR GYROKINETIC THEORY FOR FINITE-BETA PLASMAS, Physics of Fluids, 31 (1988) 1940-1948.

[13] A.J. Brizard, T.S. Hahm, Foundations of nonlinear gyrokinetic theory, Reviews of Modern Physics, 79 (2007) 421-468.
[14] Z. Lin, T.S. Hahm, W.W. Lee, W.M. Tang, R.B. White, Turbulent transport reduction by zonal flows: Massively parallel simulations, Science, 281 (1998) 1835-1837.
[15] R. Hagera, Chang, C. S., Ferraro, N. M. and Nazikian, R., Gyrokinetic understanding of the edge pedestal transport driven by resonant magnetic perturbations in a realistic divertor geometry, Physics of Plasmas, 27 (2020) 062301.
[16] W.W.W.R.B. Lee, Finite Larmor radius effects at the high confinement mode pedestal and the related force-free steady state, Physics of Plasmas, 26 (2019) 040701.
[17] Z. Lin, Y. Nishimura, Y. Xiao, I. Holod, W.L. Zhang, L. Chen, Global gyrokinetic particle simulations with kinetic electrons, Plasma Physics and Controlled Fusion, 49 (2007) B163-B172.
[18] I. Holod, W.L. Zhang, Y. Xiao, Z. Lin, Electromagnetic formulation of global gyrokinetic particle simulation in toroidal geometry, Physics of Plasmas, 16 (2009).
[19] Y. Xiao, Holod, Ihor, Wang, Zhixuan, Lin, Zhihong Lin and Zhang, Taige, Gyrokinetic particle simulation of microturbulence for general magnetic geometry and experimental profiles, 22 (2015) 022516.
[20] G. Rewoldt, Z. Lin, Y. Idomura, Linear comparison of gyrokinetic codes with trapped electrons, Computer Physics Communications, 177 (2007) 775-780.
[21] A. Brizard, NONLINEAR GYROKINETIC MAXWELL-VLASOV EQUATIONS USING MAGNETIC COORDINATES, Journal of Plasma Physics, 41 (1989) 541-559.
[22] H. Qin, W.M. Tang, G. Rewoldt, Gyrokinetic theory for arbitrary wavelength electromagnetic modes in tokamaks, Physics of Plasmas, 5 (1998) 1035-1049.
[23] H. Qin, R.H. Cohen, W.M. Nevins, X.Q. Xu, Geometric gyrokinetic theory for edge plasmas, Physics of Plasmas, 14 (2007).